Chemical Physics Letters 715 (2019) 239–243

Contents lists available at ScienceDirect

Chemical Physics Letters

journal homepage: www.elsevier.com/locate/cplett

Research paper

Model building of metal oxide surfaces and vibronic coupling density as a reactivity index: Regioselectivity of CO_2 adsorption on Ag-loaded Ga_2O_3

Yasuro Kojima[a], Wataru Ota[a,b], Kentaro Teramura[a,c], Saburo Hosokawa[a,c], Tsunehiro Tanaka[a,c], Tohru Sato[a,b,c,*]

[a] Department of Molecular Engineering, Graduate School of Engineering, Kyoto University, Nishikyo-ku, Kyoto 615-8510, Japan
[b] Fukui Institute for Fundamental Chemistry, Kyoto University, Sakyo-ku, Kyoto 606-8103, Japan
[c] Unit of Elements Strategy Initiative for Catalysts & Batteries, Kyoto University, Nishikyo-ku, Kyoto 615-8510, Japan

HIGHLIGHTS

- A step-by-step hydrogen terminated cluster model of the Ga_2O_3 surface is constructed.
- The Ag atom reacts with the Lewis basic O atom in the Ga_2O_3 cluster.
- Vibronic coupling density identifies the adsorption site of CO_2 on the Ag/Ga_2O_3.
- Adsorbed CO_2 has a bent structure.

ABSTRACT

The step-by-step hydrogen-terminated (SSHT) model is proposed as a model for the surfaces of metal oxides. Using this model, it is found that the vibronic coupling density (VCD) can be employed as a reactivity index for surface reactions. As an example, the regioselectivity of CO_2 adsorption on the Ag-loaded Ga_2O_3 photocatalyst surface is investigated based on VCD analysis. The cluster model constructed by the SSHT approach reasonably reflects the electronic structures of the Ga_2O_3 surface. The geometry of CO_2 adsorbed on the Ag-loaded Ga_2O_3 cluster has a bent structure, which is favorable for its photocatalytic reduction to CO.

1. Introduction

Heterogeneous catalysis, particularly for reactions between molecules and solid surfaces, has been extensively studied [1]. To design heterogeneous catalysts and understand of their mechanisms, the sites for molecular adsorption on the solid catalyst must be clarified. The adsorption sites can be predicted theoretically by finding the position of a molecule on a surface that has the lowest energy of all possible positions on the surface. However, it is impractical to calculate all the energies because, in general, there are many adsorption sites for a molecule on a solid surface. Therefore, a reactivity index to predict the adsorption sites based only on the information of solid surface is desirable.

Previously, we identified the regioselectivity of cycloaddition to fullerene [2–4], metallofullerene [5], and large polycyclic aromatic hydrocarbons [6] using the vibronic coupling density (VCD) as the reactivity index. Vibronic coupling, the coupling between electron and nuclear vibrations, stabilizes a system by structural relaxation after charge transfer. The VCD as a function of a position identifies the reactive sites as those where the vibronic coupling is large. It is expected that the VCD can be utilized as a reactivity index for systems with various reactive sites, such as solid surfaces.

β-Ga_2O_3 is a heterogeneous catalyst that reduces CO_2 to CO using H_2 as a reductant under photoirradiation [7,8]. The selectivity of CO_2 reduction is increased by modifying β-Ga_2O_3 with Ag, which acts as a cocatalyst [9–13]. H_2O, which is abundant, is used as the reductant in the Ag-loaded Ga_2O_3 system. In this study, we applied VCD to the Ag-loaded Ga_2O_3 surface to show the effectiveness of VCD as a reactivity index for CO_2 adsorption on the surface. This is the first report of the application of VCD to a solid surface and could provide the basis for extending the applicability of VCD to solid surfaces in general.

Reactivity indices, such as the frontier orbital density or VCD, strongly depend on the electronic structure of the frontier level. When building a model for the surface reactions of metal oxides based on a bulk crystal structure, the treatment of dangling bonds strongly affects the electronic structure. For instance, because hydrogen termination for dangling bonds involves electron doping, the frontier level is shifted by hydrogen termination. In this study, to build a model for the subsequent

* Corresponding author at: Fukui Institute for Fundamental Chemistry, Kyoto University, Takano Nishihiraki-cho 34-4, Sakyo-ku, Kyoto 606-8103, Japan.
E-mail address: tsato@scl.kyoto-u.ac.jp (T. Sato).

https://doi.org/10.1016/j.cplett.2018.11.036
Received 25 August 2018; Received in revised form 12 November 2018; Accepted 15 November 2018
Available online 24 November 2018

calculations, we employed a step-by-step hydrogen-terminated (SSHT) approach to reproduce the experimental observations.

In Section 2, we describe the theory of vibronic coupling. In Section 3, we describe the computational methods. In Section 4.1, we present a method to build a cluster model of the Ag-loaded Ga_2O_3 surface by the SSHT approach. In Section 4.2, we investigate the regioselectivity of CO_2 adsorption on Ag-loaded Ga_2O_3 cluster using VCD as the reactivity index. Finally, in Section 5, we present the conclusions of this study.

2. Theory

In the early stage of chemical reactions, charge transfer occurs between reactants by intermolecular orbital interactions. Following charge transfer, the system is further stabilized by intramolecular deformation. This structural relaxation is induced by vibronic coupling. The vibronic coupling constant (VCC) V, which quantitatively evaluates the strength of vibronic couplings, is defined by [14,15]

$$V = \left(\frac{\partial E_{CT}}{\partial \xi}\right)_{\mathbf{R}_0}, \tag{1}$$

where E_{CT} is the total energy of the charge-transfer state, and $\mathbf{R}_0$ is the equilibrium geometry before charge transfer. ξ is the reaction coordinate along the nuclear vibration that gives the largest vibronic coupling

$$\xi = \sum_{\alpha} \frac{V_\alpha}{\sqrt{\sum_\alpha |V_\alpha|^2}} Q_\alpha, \tag{2}$$

where Q_α is a normal coordinate and V_α is the VCC of vibrational mode α.

The VCD η is provided by the integrand of the VCC,

$$V = \int d^3\mathbf{r}\, \eta(\mathbf{r}). \tag{3}$$

Since $\eta(\mathbf{r})$ is a function of the spatial coordinate $\mathbf{r}$, $\eta(\mathbf{r})$ gives the local information about the VCC. The VCD can be divided into electronic and vibrational contributions:

$$\eta(\mathbf{r}) = \Delta\rho(\mathbf{r}) \times v(\mathbf{r}). \tag{4}$$

$\Delta\rho(\mathbf{r})$ is the electron density difference between neutral and charge-transfer states, and $v(\mathbf{r})$ is the potential derivative defined as the derivative of the potential acting on an electron from all the nuclei u with respect to ξ. The total differential of the chemical potential $\mu = \mu[N;u]$ which is a functional of the number of electrons N and u is given by [14]

$$d\mu = 2\zeta dN + \int \eta(\mathbf{r}) d\xi d^3\mathbf{r}, \tag{5}$$

where ζ is the absolute hardness. In terms of the chemical reactivity theory proposed by R. G. Parr and W. Yang [16,17], the preferred direction for a reagent approaching a species is the one for which the initial $|d\mu|$ is the maximum. The first term on the right-hand side of Eq. (5) is less direction sensitive than the second term. Thus, the preferred direction can be said to be that for which the $\eta(\mathbf{r})$ of a species is a maximum.

3. Computational method

For the calculations of the VCC and VCD, we first optimized the geometry of a neutral Ag-loaded Ga_2O_3 cluster and performed a vibrational analysis. Then, we calculated the forces acting on the nuclei for the neutral optimized structure in a cationic state. The charge-transfer state was chosen to be a cationic state because we assume that an electron is transferred from the Ag-loaded Ga_2O_3 surface to CO_2 in the reduction of CO_2. Finally, we determined the adsorbed structure of CO_2 on the Ag-loaded Ga_2O_3 cluster. Orbital levels were calculated with the extended Hückel theory using the geometry optimized structures by the density functional theory. The computational level was set at the B3LYP/6-31G(d,p) level for the Ga, O, and H atoms and at the B3LYP/LANL2TZ level for the Ag atom. The core electrons in the Ag atom were replaced by effective core potentials. These calculations were performed using GAUSSIAN 09 [18,19]. The VCD analysis and extended Hückel theory calculations were performed using our own code.

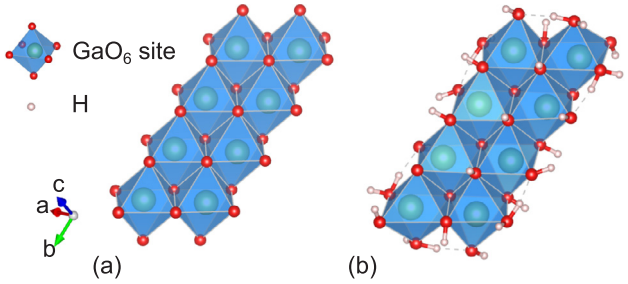

Fig. 1. Structures of the (a) bare and (b) SSHT model for the Ga_2O_3 surface where Ga atoms are located at the octahedral sites formed by O atoms.

4. Results

4.1. Cluster model of Ag-loaded Ga_2O_3 surface

β-Ga_2O_3 consists of Ga atoms located at the octahedral and tetrahedral sites formed by O atoms [20,21], as illustrated in Fig. S1 in the Supplementary Material. The octahedra share edges whereas the tetrahedra share corners in the b-axis direction. The tetrahedra also share corners with the octahedra. We expected that the electrons used for the reduction of CO_2 migrate through the octahedra shared edges. In this study, eight adjacent octahedral sites are employed as a bare cluster model of the β-Ga_2O_3 surface (Fig. 1 (a)).

Fig. 2 shows the calculated orbital levels of the bare cluster. The band gap of β-Ga_2O_3 has been experimentally estimated to be 4.6 eV [11]. However, the energy gap of the bare cluster is 0.8 eV, which is much smaller than the experimental value. This is because the occupied molecular orbitals become unoccupied when the cluster is cut from the crystal structure. The bare cluster has reactive dangling bonds arising from the cleavage of O atoms. The dangling bonds at the O atoms are terminated by H atoms because it has been experimentally observed that H atoms are adsorbed on the Ga_2O_3 surface [8]. The hydrogen termination, which involves electron doping, shifts the frontier level. The 16 unoccupied molecular orbitals must be occupied for the model to have a reasonably wide energy gap. Thus, the 32 H atoms, i.e., 2 H atoms for each unoccupied molecular orbital, are step-by-step bonded to O atoms with large molecular orbital coefficients. As a result, we

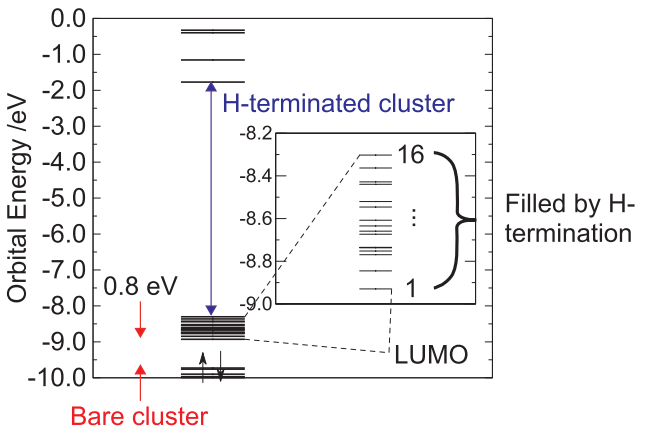

Fig. 2. Orbital levels of the bare cluster with an energy gap of 0.8 eV. Dangling bonds at the O atoms are terminated with H atoms until the cluster model has an energy gap that agrees with the experimental value.

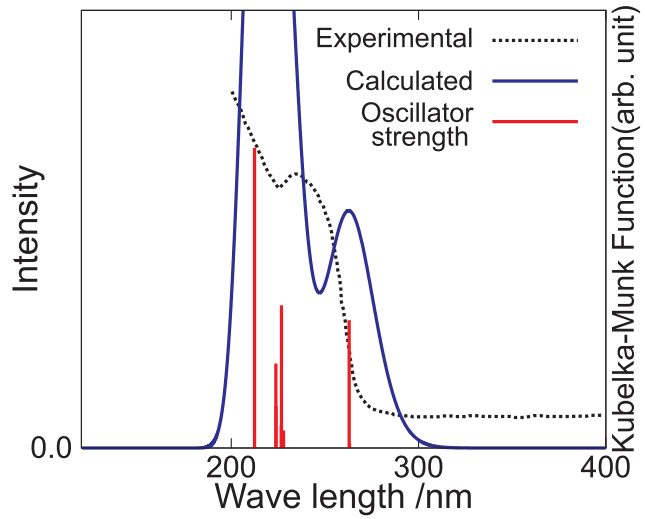

Fig. 3. Experimental (black dotted line) [11] and calculated (blue line) diffuse reflectance spectra. The red lines represent calculated oscillator strengths. (For interpretation of the references to colour in this figure legend, the reader is referred to the web version of this article.)

obtained the hydrogen-terminated cluster with an energy gap of 5.4 eV after geometry optimization. Fig. S2 in the Supplementary Material shows in detail the process of step-by-step hydrogen termination. Hereafter, we refer to this hydrogen terminated cluster as the SSHT model for the Ga_2O_3 surface. Fig. 1 (b) shows the optimized structure of the SSHT model.

The diffuse reflectance spectrum of the SSHT cluster model is evaluated to examine its reliability. The spectrum $g(x)$, which depends on the absorption energy x, is calculated from the oscillator strengths multiplied by the Gaussian distribution function,

$$g(x) = \sum_{i=1}^{10} \frac{f_i}{\sqrt{2\pi\sigma^2}} \exp\left(-\frac{(x-u_i)^2}{2\sigma^2}\right), \tag{6}$$

where f_i is the oscillator strength of a transition from S_0 to the Franck–Condon S_i states, and u_i is the excitation energy from S_0 to the Franck–Condon S_i states. The value of i is restricted between 1 and 10. The values of f_i and u_i were calculated using time-dependent density functional theory. Here, σ^2 is the variance of the Gaussian distribution function and was set to 0.05 eV^2. Fig. 3 shows a comparison of the experimental and calculated diffuse reflectance spectrum [11]. Although the calculated spectrum is shifted to the long-wavelength region with respect to the experimental spectrum, the two peaks of the calculated spectrum at 219 and 263 nm are also observed experimentally. Thus, the SSHT cluster is suitable for use as a model for the Ga_2O_3 surface.

It should be noted that, in the SSHT cluster model, H atoms are not bonded to all O atoms, although all the dangling bonds are terminated by H atoms. There are 20, 6, and 2 O atoms with which 1, 2, and 0 H atoms are bonded, respectively. The O atoms without hydrogen termination have a pair of electrons, and, thus, act as Lewis bases. This is supported by the highest occupied molecular orbital (HOMO) of the SSHT cluster model, as shown in Fig. 4 (a), which is strongly localized on the O atoms without hydrogen termination. This result indicates that these O atoms donate electrons to the reactants. The HOMO is doubly degenerate because the Lewis basic O atoms are located at both the front and back surfaces of the SSHT cluster model. Fig. 4 (b) shows the VCD of the SSHT cluster model, which is also localized on the O atoms without hydrogen termination. The stabilization arising from the structural relaxation after charge transfer is large at the sites where the VCD is localized. Therefore, the Ag-loaded Ga_2O_3 surface is modeled by placing a single Ag atom on one of the Lewis basic O atoms in the SSHT

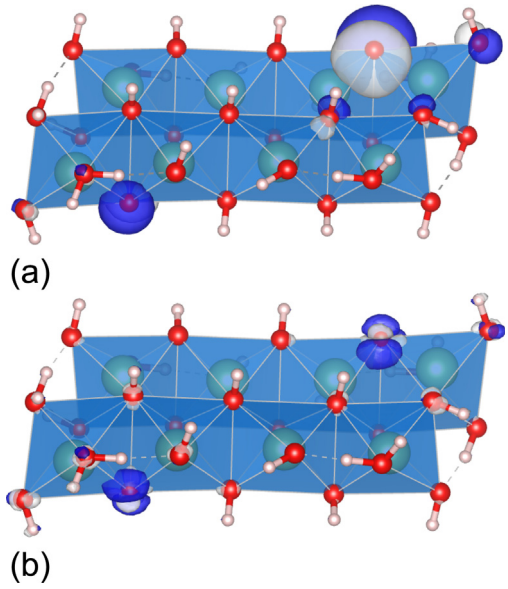

Fig. 4. (a) HOMO and (b) VCD $\eta(\mathbf{r})$ of the SSHT cluster model for the Ga_2O_3 surface. The HOMO and VCD are localized on the O atoms where H atoms are not bonded. The isosurface values of HOMO and VCD are 3.0×10^{-2} and 2.5×10^{-5} a.u., respectively.

cluster model. The Cartesian coordinates of the SSHT cluster model for the Ga_2O_3 and Ag-loaded Ga_2O_3 surfaces are given in Tables S1 and S2 of the Supplementary Material.

4.2. Regioselectivity of CO_2 adsorption on Ag-loaded Ga_2O_3 cluster

Fig. 5 shows the electron density difference $\Delta\rho(\mathbf{r})$, the potential derivative $v(\mathbf{r})$, and the VCD $\eta(\mathbf{r})$ of the Ag-loaded Ga_2O_3 cluster. Here, $\Delta\rho(\mathbf{r})$, the electron density difference between the neutral and cationic states, is delocalized around the Ag atom because the electron is mainly extracted from the Ag atom. $v(\mathbf{r})$ is large at the Ag and adjacent O atoms. Consequently, $\eta(\mathbf{r})$, which is given by the product of $\Delta\rho(\mathbf{r})$ and $v(\mathbf{r})$, is localized on the Ag atom as well as on the O atoms located near the Ag atom. Since $\eta(\mathbf{r})$ is distributed over the Ag atom and the O atoms at the surface of the Ga_2O_3 cluster, structural relaxation occurs between the Ag atom and the Ga_2O_3 cluster following charge transfer. This result implies that catalytic activity depends on the type of solid surface on which the Ag atom is loaded.

Geometry optimization is performed after the initial position of CO_2 is set above the Ag atom, as shown in Fig. 6. The adsorbed structure of CO_2 is found to have an O-C-O angle of 139° and O-C distances of 1.21

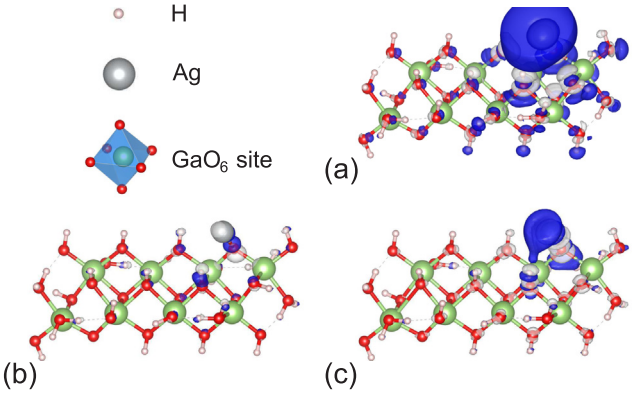

Fig. 5. (a) The electron density difference $\Delta\rho(\mathbf{r})$, (b) potential derivative $v(\mathbf{r})$, and (c) VCD $\eta(\mathbf{r})$ of the Ag-loaded Ga_2O_3 cluster. The isosurface values of $\Delta\rho(\mathbf{r})$, $v(\mathbf{r})$, and $\eta(\mathbf{r})$ are 10^{-3}, 10^{-2}, and 10^{-5} a.u., respectively.

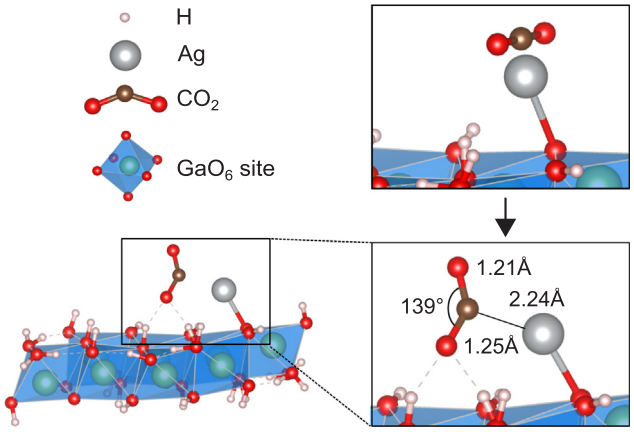

Fig. 6. Optimized structure of CO_2 on the Ag-loaded Ga_2O_3 cluster.

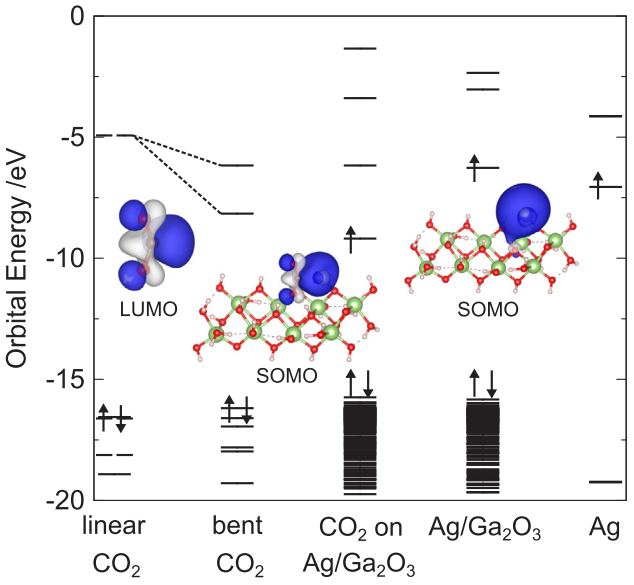

Fig. 7. Orbital levels of CO_2 on the Ag-loaded Ga_2O_3 cluster and its fragments: CO_2 and Ag-loaded Ga_2O_3 cluster. Orbital levels of the linear CO_2 and Ag atom are also shown.

and 1.25 Å. The adsorbed structure is obtained in the region where the VCD is localized. The adsorption energy of CO_2 E_{ad} is defined by

$$E_{ad} = E_{CO_2} + E_{cluster} - E_{CO_2/cluster}, \quad (7)$$

where E_{CO_2}, $E_{cluster}$, and $E_{CO_2/cluster}$ are the energies of isolated CO_2, isolated Ag-loaded Ga_2O_3 cluster, and CO_2 on the cluster, respectively. The E_{ad} of CO_2 is calculated to be 0.58 eV, indicating that the CO_2 with a bent structure is favorably adsorbed on the Ag-loaded Ga_2O_3 cluster.

Fig. 7 shows the orbital levels of CO_2 on the Ag-loaded Ga_2O_3 cluster and its fragments: CO_2 and Ag-loaded Ga_2O_3 cluster. Orbital levels of the linear CO_2 and Ag atom are also shown. The SOMO of the Ag-loaded Ga_2O_3 cluster is raised with respect to that of the Ag atom due to the interactions between the Ag atom and Ga_2O_3. The shift of the SOMO level of Ag is caused by the Ga_2O_3 support. Since the SOMO of the Ag-loaded Ga_2O_3 cluster is energetically close to the LUMO of the linear CO_2, electron transfer occurs from the Ag-loaded Ga_2O_3 to the linear CO_2. After the electron transfer, CO_2 undergoes structural relaxation from the linear structure to the bent structure. The degeneracy of LUMOs is lifted upon the structural relaxation, and the LUMO of the bent CO_2 is lower than the SOMO of the Ag-loaded Ga_2O_3. This enhances the occupation of the antibonding LUMO of CO_2 by photo-excited electrons transferred from photo-irradiated Ga_2O_3, which weakens the bond between C and O atoms. A similar orbital diagram is obtained for a Cu-loaded Ga_2O_3 cluster model. The orbital diagrams of the Cu-loaded Ga_2O_3 cluster and CO_2 are shown in Fig. S4 in the Supplementary Material. Therefore, Ga_2O_3 loaded with a metal atom with its SOMO close to the LUMO of CO_2 such as Ag or Cu would be favorable for CO_2 reduction. In this study, the Ag and Cu are supposed to be loaded as a single atom. As shown in Fig. S5 in the Supplementary Material, the orbital diagrams of the Ag clusters exhibit a complex behavior. Therefore, the size effect of the Ag clusters would not be monotonous.

Geometry optimizations are performed by changing the initial positions of CO_2 to examine the dependence of the adsorbed structure. The initial positions of CO_2 are prepared such that CO_2 surrounds the Ag atom where $\Delta\rho(\mathbf{r})$ is distributed. Although $\Delta\rho(\mathbf{r})$ can also be used as a reactivity index, it tends to be delocalized compared to the VCD. Fig. 8 shows the optimized structures obtained for each initial CO_2 position. Optimized structures 1 and 2 in Fig. 8 are the same as that in Fig. 6. In structures 3 and 4, CO_2 has a linear structure that is unfavorable for the reduction of CO_2. Furthermore, the E_{ad} of CO_2 for structures 3 and 4 are calculated to be 0.47 and 0.30 eV, respectively. These values are smaller than the values of E_{ad} for structures 1 and 2 of 0.58 eV. Therefore, the adsorption of CO_2 in the region where the VCD is localized is advantageous for the CO_2 reduction, as well as being the most stable of the optimized structures. Consequently, the regioselectivity of CO_2 adsorption is clearly indicated by the VCD because of the considerations of the vibronic contribution to the stabilization of the system in contrast to $\Delta\rho(\mathbf{r})$, which only considers the electronic contribution. As shown in Fig. S3 of the Supplementary Material, the optimized structures obtained by placing CO_2 on Ga atoms are energetically unstable compared to the structure obtained by the VCD analysis.

5. Conclusion

A cluster model of the Ga_2O_3 photocatalyst surface is constructed by terminating dangling bonds with H atoms. The H atoms are bonded to O atoms with large orbital coefficients for each unoccupied orbitals such that the cluster model has an energy gap in agreement with the experimental values. The O atoms without hydrogen termination act as Lewis bases. This process of building a cluster model for metal oxide surfaces is termed as the step-by-step hydrogen-terminated (SSHT)

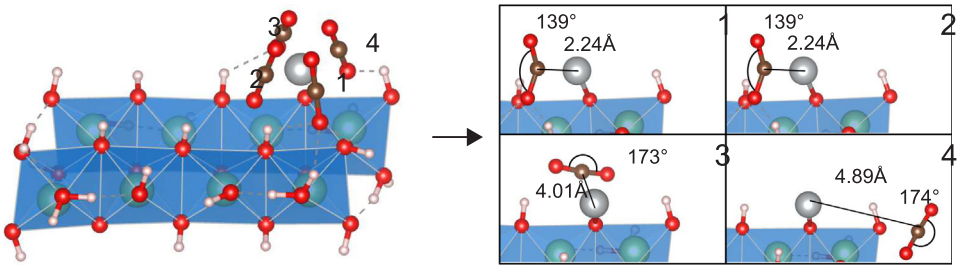

Fig. 8. Optimized structures obtained by changing the initial positions of CO_2 such that CO_2 surrounds the Ag atom.

approach. The vibronic coupling density (VCD) of the Ag-loaded Ga_2O_3 cluster is evaluated to identify the adsorption sites for CO_2. Thus, the VCD is an effective reactivity index for determining the regioselectivity of CO_2 adsorption on the Ag-loaded Ga_2O_3 surface. We also found that CO_2 with a bent structure, which is advantageous for photocatalytic reduction, is adsorbed on the Ag atom.

Acknowledgments

This work was supported by the Elements Strategy Initiative for Catalysts and Batteries (ESICB). The calculations were partly performed using the Supercomputer Laboratory of Kyoto University and Research Center for Computational Science, Okazaki, Japan.

Appendix A. Supplementary material

Supplementary data associated with this article can be found, in the online version, at https://doi.org/10.1016/j.cplett.2018.11.036.

References

[1] G. Ertl, H. Knözinger, F. Schüth, J. Weitkamp, Handbook of Heterogeneous Catalysis, second ed., Wiley-VCH, Weinheim, 2008.
[2] N. Haruta, T. Sato, K. Tanaka, J. Org. Chem. 77 (2012) 9702.
[3] T. Sato, N. Iwahara, N. Haruta, K. Tanaka, Chem. Phys. Lett. 531 (2012) 257.
[4] N. Haruta, T. Sato, K. Tanaka, Tetrahedron 70 (2014) 3510.
[5] N. Haruta, T. Sato, K. Tanaka, J. Org. Chem. 80 (1) (2014) 141.
[6] N. Haruta, T. Sato, K. Tanaka, Tetrahedron Lett. 56 (4) (2015) 590.
[7] K. Teramura, H. Tsuneoka, T. Shishido, T. Tanaka, Chem. Phys. Lett. 467 (2008) 191.
[8] H. Tsuneoka, K. Teramura, T. Shishido, T. Tanaka, J. Phys. Chem. C 114 (2010) 8892.
[9] K. Teramura, Z. Wang, S. Hosokawa, Y. Sakata, T. Tanaka, Chem. Eur. J. 20 (2014) 9906.
[10] Z. Wang, K. Teramura, S. Hosokawa, T. Tanaka, J. Mater. Chem. A 3 (2015) 11313.
[11] Z. Wang, K. Teramura, Z. Huang, S. Hosokawa, Y. Sakata, T. Tanaka, Catal. Sci. Technol. 6 (2016) 1025.
[12] M. Yamamoto, T. Yoshida, N. Yamamoto, T. Nomoto, Y. Yamamoto, S. Yagi, H. Yoshida, J. Mater. Chem. A 3 (2015) 16810.
[13] Y. Kawaguchi, M. Akatsuka, M. Yamamoto, K. Yoshioka, A. Ozawa, Y. Kato, T. Yoshida, J. Photochem. Photobiol. A 358 (2018) 459.
[14] T. Sato, K. Tokunaga, K. Tanaka, J. Phys. Chem. A 112 (2008) 758.
[15] T. Sato, K. Tokunaga, N. Iwahara, K. Shizu, K. Tanaka, H. Köppel, D.R. Yarkony, H. Barentzen (Eds.), Vibronic Coupling Constant and Vibronic Coupling Density in The Jahn-Teller Effect: Fundamentals and Implications for Physics and Chemistry, Springer-Verlag, Berlin and Hidelberg, 2009.
[16] R.G. Parr, W. Yang, J. Am. Chem. Soc. 106 (1984) 4049.
[17] R.G. Parr, W. Yang, Density-Functional Theory of Atoms and Molecules, Oxford University Press, New York, 1994.
[18] M.J. Frisch, et al., Gaussian 09, Revision D. 01, Gaussian, Inc., Wallingford CT, 2013.
[19] M.J. Frisch, et al., Gaussian 09, Revision E. 01, Gaussian, Inc., Wallingford CT, 2013.
[20] S. Geller, J. Chem. Phys. 33 (1960) 676.
[21] J. Åhman, G. Svensson, J. Albertsson, Acta Cryst. C 52 (1996) 1336.